

An inexact proximal majorization-minimization Algorithm for remote sensing image stripe noise removal

Chengjing Wang · Xile Zhao · Qingsong
Wang · Zepei Ma · Peipei Tang

Received: date / Accepted: date

Abstract The stripe noise existing in remote sensing images badly degrades the visual quality and restricts the precision of data analysis. Therefore, many destriping models have been proposed in recent years. In contrast to these existing models, in this paper, we propose a nonconvex model with a DC function (i.e., the difference of convex functions) structure to remove the strip noise. To solve this model, we make use of the DC structure and apply an inexact proximal majorization-minimization algorithm with each inner subproblem solved by the alternating direction method of multipliers. It deserves mentioning that we design an implementable stopping criterion for the inner subproblem, while the convergence can still be guaranteed. Numerical experiments demonstrate the superiority of the proposed model and algorithm.

Keywords Remote sensing · group sparsity · proximal majorization-minimization algorithm · alternating direction method of multipliers

Mathematics Subject Classification (2020) 65K05 · 90C26 · 90C90

Chengjing Wang
School of Mathematics, Southwest Jiaotong University E-mail: renaissance-wang@hotmail.com

Xile Zhao
School of Mathematical Sciences/Research Center for Image and Vision Computing, University of Electronic Science and Technology of China E-mail: xlzhao122003@163.com

Qingsong Wang
Department of Mathematics, National University of Defense Technology E-mail: nothing2wang@hotmail.com

Zepei Ma
School of Mathematics, Southwest Jiaotong University E-mail: 2900675707@qq.com

Peipei Tang (corresponding author)
Hangzhou City University, E-mail: tangpp@hzcu.edu.cn

1 Introduction

Nowadays, remote sensing images are playing an important role in the environment, agriculture, biology, mineralogy, and so on. One may see [14], [21], [13] for more details. Due to the limitation of sensors, remote sensing images are inevitably corrupted by noise, which deteriorates the quality of remote sensing images and hinders their subsequent applications (e.g., classification [12] and detection [9]). Remote sensing image denoising (RSID), which removes the noise while preserving the details and edges, is one of the fundamental problems in remote sensing image processing and analysis [14].

In this work, we mainly focus on the stripe noise scenario. The degradation process [4], [17], can be mathematically formulated as

$$f(x, y) = u(x, y) + s(x, y), \quad (1)$$

where $f(x, y)$, $u(x, y)$ and $s(x, y)$ represent the degraded image from the detector, the potential fringeless image, and the fringe component at (x, y) , respectively. In order to discuss the numerical algorithm, the matrix vector form of (1) can be rewritten as follows

$$f = u + s, \quad (2)$$

where f , u and s represent the vectorized discrete versions of $f(x, y)$, $u(x, y)$ and $s(x, y)$, respectively.

- (1) Directionality: consider the gradient of fringe components in horizontal and vertical directions. Here, we use the convex function 1-norm as the sparse regularization and give

$$R_1(s) = \|\nabla_y s\|_{1,1},$$

where ∇_y denotes a linear first order difference operator in the vertical direction.

The horizontal gradient of the desired image u should be smooth. Therefore, the one-way total change [4] of the desired image is considered to be

$$R_2(s) = \|\nabla_x u\|_1 = \|\nabla_x f - \nabla_x s\|_{1,1},$$

where ∇_x denotes the first order difference operator in the horizontal direction.

- (2) Structural properties: moreover, different from the random noise, the fringe component shows a special columnar structure. Therefore, the regular term [6] is designed as

$$R_3(s) = \|s\|_{2,1},$$

where $\|s\|_{2,1} = \sum_{j=1}^n \left(\sum_{i=1}^m s_{i,j}^2 \right)^{\frac{1}{2}}$, $\forall s \in \mathbb{R}^{m \times n}$.

Based on the above analysis, the stripe component has significant directionality and structure. By combining R_1 , R_2 and R_3 , Chen et al. [6] proposed the fringe noise removal model as follows

$$\min_s \{\lambda_1 \|\nabla_y s\|_{1,1} + \lambda_2 \|\nabla_x f - \nabla_x s\|_{1,1} + \lambda_3 \|s\|_{2,1}\}, \quad (3)$$

where λ_1 , λ_2 and λ_3 are three positive regularization parameters that balance the three terms.

In order to simplify the sign, we abbreviate $p_1(s) = \lambda_1 \|\nabla_y s\|_{1,1}$, $p_2(u) = \lambda_2 \|\nabla_x f - \nabla_x u\|_{1,1}$ and $p_3(v) = \lambda_3 \|v\|_{2,1} = \lambda_3 \|h(v)\|_1$ with $(h(v))_i := \|v(:, i)\|$. So (3) is rewritten as follows

$$\min_s \{p_1(s) + p_2(s) + p_3(s)\}. \quad (4)$$

For the convenience of discussion, each stripe line is regarded as a column. If the stripes are horizontal, rotate them so that the stripe lines are vertical. When the fringe component is extracted from the fringe image, the final denoising image can be estimated by the following formula

$$u = f - s.$$

Fan and Li [11] proposed a nonconvex sparsity function called SCAD as a surrogate of the ℓ_0 function, which has been used as the regularizer to avoid the model overfitting in high-dimensional statistical learning. It can achieve a sparse estimation with fewer measurements, faster convergence and furthermore is more robust against noises. In this paper, we apply the SCAD function to substitute the ℓ_1 function part in the model (4) in order to remove the noise more well. Hence the considered model becomes a nonconvex model. In the computational aspect, we adopt an inexact proximal majorization-minimization (PMM) algorithm to solve the nonconvex model with each inner subproblem solved by the dual alternating direction method (dADMM). Although Tang et al. [19] proposed the PMM algorithm to solve the nonconvex square-root-loss regression problems and the inner subproblem is also solved inexactly by the semismooth Newton method, the stopping criterion for the inner subproblem is not implementable and remains on the theoretical level. Tang, Wang and Jiang [18] proposed the proximal-proximal majorization-minimization (PPMM) algorithm to solve the nonconvex rank regression problems with each inner subproblem solved by the semismooth Newton method. They proposed a stopping criterion for the inner subproblem, however, the convergence analysis is relatively easier since the considered problem is polyhedral and the inner subproblem is an unconstrained one. Numerical experiments demonstrate that the modified model and the proposed algorithm is more competitive.

The remaining parts of this paper are organized as follows. In Section 2, we introduce some basic concepts and preliminary results. In Section 3, we set up the model problem and present the details of the algorithm. In Section 4, we analyze the convergence of the proposed algorithm. In Section 5, we

implement the numerical experiments to compare our model with the original convex model and also compare our algorithm with the existing algorithms. We conclude our paper in Section 6.

2 Preliminaries

In this section, we introduce some preliminaries that will be used in this paper.

Let \mathbb{X} and \mathbb{Y} be finite dimensional Hilbert spaces. For any convex function $f : \mathbb{X} \rightarrow (-\infty, +\infty]$, the conjugate function of f is defined as

$$f^*(y) := \sup_{x \in \text{dom}(f)} \left\{ \langle y, x \rangle - f(x) \right\}.$$

For a closed proper convex function $f : \mathbb{X} \rightarrow (-\infty, +\infty]$ and a parameter $\sigma > 0$, the proximal mapping $\text{Prox}_{\sigma f}$ is defined as

$$\text{Prox}_{\sigma f}(y) := \arg \min_x \left\{ f(x) + \frac{1}{2\sigma} \|y - x\|^2 \right\}, \forall y \in \mathbb{X}.$$

The proximal mapping $\text{Prox}_{\sigma f}$ is single-valued and continuous with the following Moreau identity (see e.g., [16, Theorem 31.5]) holds

$$\text{Prox}_{\sigma f}(x) + \sigma \text{Prox}_{\frac{1}{\sigma} f^*} \left(\frac{1}{\sigma} x \right) = x.$$

A multifunction $\mathcal{F} : \mathbb{X} \rightrightarrows \mathbb{Y}$ is locally upper Lipschitz continuous at $x \in \mathbb{X}$ if there exist a parameter κ which is independent of x and a neighbourhood \mathcal{U} of x such that $\mathcal{F}(y) \subseteq \mathcal{F}(x) + \kappa \|y - x\| \mathbb{B}_{\mathbb{X}}$ holds for any $y \in \mathcal{U}$, where $\mathbb{B}_{\mathbb{X}}$ is a unit ball of the space \mathbb{X} . The multifunction \mathcal{F} is said to be piecewise polyhedral if its graph $\text{gph} \mathcal{F} := \{(x, y) \mid y \in \mathcal{F}(x)\}$ is the union of finitely many polyhedral convex sets.

The Kurdyka-Łojasiewicz (KL) property (see e.g., [3]) plays a central role in the convergence analysis. For further discussion, we introduce this concept below.

Definition 1 A proper lower semicontinuous function $r : \mathbb{X} \rightarrow (-\infty, +\infty]$ is said to have the KL property at $x \in \text{dom}(\partial r)$ if there exist $\eta \in (0, +\infty]$, a neighbour \mathcal{U} of x and a continuous concave function $\varphi : [0, \eta) \rightarrow [0, +\infty)$ satisfying

- (1) $\varphi(0) = 0$;
 - (2) φ is continuous at 0 and continuously differentiable on $(0, \eta)$;
 - (3) $\varphi'(s) > 0$, for all $0 < s < \eta$
- such that the KL inequality $\varphi'(r(x') - r(x)) \text{dist}(0, \partial r(x')) \geq 1$ holds for any $x' \in \mathcal{U}$ and $r(x) < r(x') < r(x) + \eta$. If r satisfies the KL property at each point of $\text{dom}(\partial r)$, then r is called a KL function.

3 Problem setup and the algorithm

In this paper, we consider the following nonconvex model problem by employing the SCAD function instead of (4)

$$\min_s \left\{ g(s) := p_1(s) - q_1(s) + p_2(s) - q_2(s) + p_3(s) - q_3(s) \right\}, \quad (5)$$

where $q_1(s) = q_{\alpha, \lambda_1}(\nabla_y s)$, $q_2(u) = q_{\alpha, \lambda_2}(\nabla_x u)$ and $q_3(v) = q_{\alpha, \lambda_3}(h(v))$, here

$$q_{\alpha, \lambda}(x) = \sum_{i=1}^n q^{\text{scad}}(x_i; \alpha, \lambda), \quad q^{\text{scad}}(t; \alpha, \lambda) = \begin{cases} 0, & \text{if } |t| \leq \lambda, \\ \frac{(|t| - \lambda)^2}{2(\alpha - 1)}, & \text{if } \lambda \leq |t| \leq \alpha\lambda, \\ \lambda|t| - \frac{\alpha + 1}{2}\lambda^2, & \text{if } |t| > \alpha\lambda. \end{cases}$$

In the above formula, we take $\alpha = 3.7$ in both the theoretical analysis and the numerical implementation. Note that the function $q_{\alpha, \lambda}(x)$ is continuously differentiable with

$$\frac{\partial q_{\alpha, \lambda}(x)}{\partial x_i} = \begin{cases} 0, & \text{if } |x_i| \leq \lambda, \\ \frac{\text{sign}(x_i)(|x_i| - \lambda)}{\alpha - 1}, & \text{if } \lambda < |x_i| \leq \alpha\lambda, \\ \lambda \text{sign}(x_i), & \text{if } |x_i| > \alpha\lambda. \end{cases}$$

3.1 The inexact PMM for the problem (5)

In this subsection, we present the framework of the inexact PMM. For simplicity, we write the problem (5) as

$$\min_s \left\{ P(s) - Q(s) \right\}, \quad (6)$$

where $P(s) = p_1(s) + p_2(s) + p_3(s)$, $Q(s) = q_1(s) + q_2(s) + q_3(s)$.

Although problem (6) is nonconvex, it is in a DC form. Thus, we naturally linearize the latter convex term $Q(s)$ to transform a nonconvex problem to a convex one, add a proximal term to guarantee the strong convexity, then adopt the sequential convexification approach to solve the problem. Now we present the algorithm as follows.

Algorithm 1 The inexact PMM for the problem (6):

Choose s^0 . For $k = 0, 1, 2, \dots$, iterate:

1. Compute s^{k+1}

$$s^{k+1} \approx \arg \min_s \left\{ P(s) - Q(s^k) - \langle \nabla Q(s^k), s - s^k \rangle + \frac{1}{2\tilde{\sigma}_k} \|s - s^k\|^2 \right\}. \quad (7)$$

2. If a stopping criterion is not satisfied, go to **Step 1**.

3.2 The dADMM for the subproblem (7)

In this subsection, we focus on how to solve the subproblem (7). In the problem (7), for $q_i(x)$ ($i = 1, 2, 3$), at the k th iteration we have $q_i(x) \geq q_i(x^k) + \langle g_i^k, x - x^k \rangle$, where $g_i^k := \nabla q_i(x^k)$. We denote $\widehat{p}_1(s) := p_1(s) + \frac{1}{2\sigma_k} \|s - s^k\|^2$ and $\widehat{p}_3(v) := \lambda_3 \|h(v)\| - \langle g_h^k, h(v) \rangle$, where $g_h^k := \nabla q_3(h(v^k))$. By introducing two variables u and v , the problem (7) can be equivalently rewritten as

$$\begin{aligned} & \min_{s,u,v} \widehat{p}_1(s) - \langle g_1^k, s \rangle + p_2(u) - \langle g_2^k, u \rangle + \widehat{p}_3(v) \\ \text{s.t.} \quad & f - s - u = 0, \\ & s - v = 0. \end{aligned} \quad (8)$$

The Lagrangian function associated with the problem (8) is given by

$$l(s, u, v; x, y) = \widehat{p}_1(s) - \langle g_1^k, s \rangle + p_2(u) - \langle g_2^k, u \rangle + \widehat{p}_3(v) + \langle x, u + s - f \rangle + \langle y, v - s \rangle.$$

Then the Karush-Kuhn-Tucker (KKT) condition for the problem (8) is

$$\begin{aligned} f - s - u = 0, \quad s - v = 0, \quad s - \text{Prox}_{\widehat{p}_1}(s + g_1^k - x + y) = 0, \\ u - \text{Prox}_{p_2}(u + g_2^k - x) = 0, \quad v - \text{Prox}_{\widehat{p}_3}(v - y) = 0. \end{aligned} \quad (9)$$

And the dual problem is

$$\begin{aligned} & \min_{x,y,z,\widehat{x},\widehat{y}} \widehat{p}_1^*(z) + p_2^*(\widehat{x}) + \widehat{p}_3^*(\widehat{y}) + \langle x, f \rangle \\ \text{s.t.} \quad & -x + y + g_1^k = z, \\ & -x + g_2^k = \widehat{x}, \\ & -y = \widehat{y}. \end{aligned} \quad (10)$$

Next, the augmented Lagrangian function associated with the problem (10) is

$$\begin{aligned} L_\sigma(x, y, z, \widehat{x}, \widehat{y}; s, u, v) = & \widehat{p}_1^*(z) + p_2^*(\widehat{x}) + \widehat{p}_3^*(\widehat{y}) + \langle x, f \rangle + \frac{\sigma}{2} \| -x + y + g_1^k - z + \frac{1}{\sigma} s \|^2 \\ & + \frac{\sigma}{2} \| -x + g_2^k - \widehat{x} + \frac{1}{\sigma} u \|^2 + \frac{\sigma}{2} \| -y - \widehat{y} + \frac{1}{\sigma} v \|^2 \\ & - \frac{1}{2\sigma} (\|s\|^2 + \|u\|^2 + \|v\|^2). \end{aligned}$$

Then we describe the details of how to solve the subproblems.

- (1) **(x, y) -subproblem:** Let (\bar{x}, \bar{y}) denote the optimal solution of the (x, y) -subproblem, i.e.,

$$(\bar{x}, \bar{y}) = \arg \min_{x,y} \left\{ L_\sigma(x, y, z, \widehat{x}, \widehat{y}; s, u, v) \right\}.$$

It is equivalent to solving the following linear system of equations

$$\begin{bmatrix} 2I & -I \\ -I & 2I \end{bmatrix} \begin{bmatrix} x \\ y \end{bmatrix} = \frac{1}{\sigma} \begin{bmatrix} s + u - f - \sigma(z + \widehat{x} - g_1^k - g_2^k) \\ v - s + \sigma(z - \widehat{y} - g_1^k) \end{bmatrix}.$$

(2) (z, \hat{x}, \hat{y}) -**subproblem:** Let $(\bar{z}, \bar{x}, \bar{y})$ be the optimal solution of the (z, \hat{x}, \hat{y}) -subproblem. We have

$$\begin{aligned}\bar{z} &= \arg \min_z \left\{ \hat{p}_1^*(z) + \frac{\sigma}{2} \left\| -x + y + g_1^k - z + \frac{1}{\sigma} s \right\|^2 \right\} \\ &= \text{Prox}_{\frac{1}{\sigma} \hat{p}_1^*} \left(\frac{s}{\sigma} - x + y + g_1^k \right), \\ \bar{x} &= \arg \min_{\hat{x}} \left\{ p_2^*(\hat{x}) + \frac{\sigma}{2} \left\| -x + g_2^k - \hat{x} + \frac{1}{\sigma} u \right\|^2 \right\} \\ &= \text{Prox}_{\frac{1}{\sigma} p_2^*} \left(\frac{u}{\sigma} - x + g_2^k \right), \\ \bar{y} &= \arg \min_{\hat{y}} \left\{ \hat{p}_3^*(\hat{y}) + \frac{\sigma}{2} \left\| -y - \hat{y} + \frac{1}{\sigma} v \right\|^2 \right\} \\ &= \text{Prox}_{\frac{1}{\sigma} \hat{p}_3^*} \left(\frac{v}{\sigma} - y \right).\end{aligned}$$

Based on the Moreau identity, we have

$$\begin{aligned}\text{Prox}_{\frac{1}{\sigma} \hat{p}_1^*} \left(\frac{s}{\sigma} - x + y + g_1^k \right) &= \frac{1}{\sigma} (s - \sigma x + \sigma y + \sigma g_1^k - \text{Prox}_{\sigma \hat{p}_1} (s - \sigma x + \sigma y + \sigma g_1^k)), \\ \text{Prox}_{\frac{1}{\sigma} p_2^*} \left(\frac{u}{\sigma} - x + g_2^k \right) &= \frac{1}{\sigma} (u - \sigma x + \sigma g_2^k - \text{Prox}_{\sigma p_2} (u - \sigma x + \sigma g_2^k)), \\ \text{Prox}_{\frac{1}{\sigma} \hat{p}_3^*} \left(\frac{v}{\sigma} - y \right) &= \frac{1}{\sigma} (v - \sigma y - \text{Prox}_{\sigma \hat{p}_3} (v - \sigma y)).\end{aligned}$$

Note that

$$\begin{aligned}\text{Prox}_{\sigma \hat{p}_1} (s) &= \arg \min_x \left\{ \|\nabla_y x\|_1 + \frac{1}{2\tilde{\sigma}_k} \|x - s^k\|^2 + \frac{1}{2\sigma} \|x - s\|^2 \right\} \\ &= \arg \min_x \left\{ \|\nabla_y x\|_1 + \frac{1}{2\hat{\sigma}} \|x - \hat{s}\|^2 \right\} \\ &= \text{Prox}_{\hat{\sigma} p_1} (\hat{s}),\end{aligned}\tag{11}$$

where $\hat{\sigma} = \sigma \tilde{\sigma}_k / (\sigma + \tilde{\sigma}_k) < \sigma$, $\hat{s} = \hat{\sigma} (s/\sigma + s^k/\tilde{\sigma}_k)$.

As we know, for $s_v \in \mathbb{R}^n$, $\lambda > 0$, let $\|\nabla \cdot\|_1$ denote the first order difference operator of a vector, then the proximal mapping of $\|\nabla \cdot\|_1$

$$\text{Prox}_{\lambda \|\nabla \cdot\|_1} (s_v) = \arg \min_{x \in \mathbb{R}^n} \left\{ \|\nabla x_v\|_1 + \frac{1}{2\lambda} \|x_v - s_v\|^2 \right\}\tag{12}$$

can be obtained by the fast algorithm proposed by Condat [7]. Hence, $\text{Prox}_{\hat{\sigma} p_1} (\hat{s})$ in (11) can be computed column by column via (12), i.e.,

$$\begin{aligned}\text{Prox}_{\sigma \hat{p}_3} (s) &= \arg \min_v \left\{ \hat{p}_3(v) + \frac{1}{2\sigma} \|v - s\|^2 \right\} \\ &= \arg \min_v \left\{ \lambda_1 \|h(v)\|_1 - \langle g_h^k, h(v) \rangle + \frac{1}{2\sigma} \|v - s\|^2 \right\},\end{aligned}\tag{13}$$

where $h(v)$ is a vector defined in Section 1. Due to the separability of $\|\cdot\|_1$ and $\|\cdot\|^2$, we can solve the problem (13) in the following separate form

$$v(:, i) = \arg \min_{v(:, i)} \left\{ (\lambda_1 - (g_h^k)_i) \|v(:, i)\| + \frac{1}{2\sigma} \|v(:, i) - s(:, i)\|^2 \right\}, \quad i = 1, \dots, n, \quad (14)$$

where $(g_h^k)_i$ is the i th element of the vector g_h^k . Since we take $\alpha = 3.7$ in the SCAD function, we have $\lambda_1 - (g_h^k)_i > 0$, which guarantees that the problem (14) is convex.

Now, we describe the dADMM for the problem (10) as follows.

Algorithm 2 The dADMM for the problem (10):

Let $\tau \in (0, (1 + \sqrt{5})/2)$ be a scalar parameter, $\sigma > 0$ be a given parameter, and choose $\{x^0, y^0, z^0, \hat{x}^0, \hat{y}^0, s^0, u^0, v^0\}$. For $j = 0, 1, 2, \dots$, iterate:

1. Solve the following linear system to compute (x^{j+1}, y^{j+1}) :

$$\begin{bmatrix} 2I & -I \\ -I & 2I \end{bmatrix} \begin{bmatrix} x^{j+1} \\ y^{j+1} \end{bmatrix} = \frac{1}{\sigma} \begin{bmatrix} s^j + u^j - f - \sigma(z^j + \hat{x}^j - g_1^k - g_2^k) \\ v^j - s^j + \sigma(z^j - \hat{y}^j - g_1^k) \end{bmatrix}.$$

2. Compute $(\hat{x}^{j+1}, \hat{y}^{j+1}, z^{j+1})$:

$$\begin{bmatrix} \hat{x}^{j+1} \\ \hat{y}^{j+1} \\ z^{j+1} \end{bmatrix} = \begin{bmatrix} \text{Prox}_{\frac{1}{\sigma} p_2^*}(\frac{1}{\sigma} u^j - x^{j+1} + g_2^k) \\ \text{Prox}_{\frac{1}{\sigma} \hat{p}_3^*}(\frac{1}{\sigma} v^j - y^{j+1}) \\ \text{Prox}_{\frac{1}{\sigma} \hat{p}_1^*}(\frac{1}{\sigma} s^j - x^{j+1} + y^{j+1} + g_1^k) \end{bmatrix}.$$

3. Update $(s^{j+1}, u^{j+1}, v^{j+1})$:

$$\begin{aligned} s^{j+1} &= s^j + \tau \sigma (-x^{j+1} + y^{j+1} + g_1^k - z^{j+1}), \\ u^{j+1} &= u^j + \tau \sigma (-x^{j+1} + g_2^k - \hat{x}^{j+1}), \\ v^{j+1} &= v^j + \tau \sigma (-y^{j+1} - \hat{y}^{j+1}). \end{aligned}$$

4. If a stopping criterion is not satisfied, go to **Step 1**.

4 Convergence Analysis

In this section, we analyze the convergence of the algorithm.

4.1 Convergence analysis for the inexact dADMM

Since the inexact dADMM for the inner subproblem can be regarded as a special case of the inexact symmetric Gauss-Seidel method [5], the convergence analysis can also be borrowed to here.

Theorem 1 *Suppose that the solution set to the KKT system (9) is nonempty and the sequence $\{(s^j, w^j, v^j, x^j, y^j, z^j, \hat{x}^j, \hat{y}^j)\}$ is generated by the dADMM, then $\{(s^j, w^j, v^j)\}$ converges to the solution of the primal problem (8) and $\{(x^j, y^j, z^j, \hat{x}^j, \hat{y}^j)\}$ converges to the solution of the dual problem (10).*

4.2 Convergence analysis for the PMM algorithm

In this subsection, we focus on the convergence analysis of the PMM algorithm. Since the inner subproblem is solved inexactly, the error must be considered if analyzing the convergence of the PMM algorithm. When solving the subproblem (10), we actually solve the following problem

$$\begin{aligned} \min_{x, y, z, \hat{x}, \hat{y}} & \left\{ \widehat{p}_1^*(z + r_z^{k+1}) + p_2^*(\hat{x} + r_{\hat{x}}^{k+1}) + \widehat{p}_3^*(\hat{y} + r_{\hat{y}}^{k+1}) + \langle x, f \rangle + \right. \\ & \left. \langle x, r_x^{k+1} \rangle + \langle y, r_y^{k+1} \rangle + \langle z, r_z^{k+1} \rangle + \langle \hat{x}, r_{\hat{x}}^{k+1} \rangle + \langle \hat{y}, r_{\hat{y}}^{k+1} \rangle \right\} \\ \text{s.t.} & \quad -x + y + g_1^k - z - r_1^{k+1} = 0, \\ & \quad -x + g_2^k - \hat{x} - r_2^{k+1} = 0, \\ & \quad -y - \hat{y} - r_3^{k+1} = 0, \end{aligned} \quad (15)$$

where $r_1^{k+1}, r_2^{k+1}, r_3^{k+1}, r_x^{k+1}, r_y^{k+1}, r_z^{k+1}, r_{\hat{x}}^{k+1}, r_{\hat{y}}^{k+1} \in \mathbb{R}^{m \times n}$ are error matrices. Therefore, the original primal problem we actually solve is

$$\begin{aligned} \min_s & \left\{ \widehat{p}_1(s - r_z^{k+1}) + p_2(f - s + r_x - r_{\hat{x}}^{k+1}) + \widehat{p}_3(s + r_y^{k+1} - r_{\hat{y}}^{k+1}) - \right. \\ & \langle s, g_1^k - r_1^{k+1} \rangle - \langle f - s + r_x^{k+1}, g_2^k - r_2^{k+1} \rangle - \langle s + r_y^{k+1}, -r_3^{k+1} \rangle - \\ & \left. \langle r_z^{k+1}, s - r_z^{k+1} \rangle - \langle r_{\hat{x}}^{k+1}, f - s + r_x^{k+1} - r_{\hat{x}}^{k+1} \rangle - \langle r_{\hat{y}}^{k+1}, s + r_y^{k+1} - r_{\hat{y}}^{k+1} \rangle \right\}. \end{aligned} \quad (16)$$

Let $r^{k+1} := (r_1^{k+1}, r_2^{k+1}, r_3^{k+1}, r_x^{k+1}, r_y^{k+1}, r_z^{k+1}, r_{\hat{x}}^{k+1}, r_{\hat{y}}^{k+1}) \in \mathbb{R}^{m \times n}$. Note that r^{k+1} converges to zero, it follows that if the inner subproblem is adequately iterated, then r^{k+1} satisfies

$$\begin{aligned} & 2p_1(r_z^{k+1}) + 2p_2(r_x^{k+1} - r_{\hat{x}}^{k+1}) + 2p_3(r_y^{k+1} - r_{\hat{y}}^{k+1}) \\ & + \frac{1}{2\tilde{\sigma}_k} \|r_z^{k+1}\|^2 + \text{pert}(r^{k+1}) \leq \frac{1}{4\tilde{\sigma}_k} \|s^{k+1} - s^k\|^2, \end{aligned} \quad (17)$$

where

$$\begin{aligned} \text{pert}(r^{k+1}) := & |\langle s, r_1^{k+1} \rangle + \langle f - s + r_x^{k+1}, r_2^{k+1} \rangle + \langle s + r_y^{k+1}, r_3^{k+1} \rangle + \langle r_z^{k+1}, s - r_z^{k+1} \rangle \\ & + \langle r_{\hat{x}}^{k+1}, f - s + r_x^{k+1} - r_{\hat{x}}^{k+1} \rangle + \langle r_{\hat{y}}^{k+1}, s + r_y^{k+1} - r_{\hat{y}}^{k+1} \rangle|. \end{aligned}$$

In the following, for the convenience of statement, we denote

$$\begin{aligned} f_k(s) := & \widehat{p}_1(s - r_z^{k+1}) + p_2(f - s + r_x^{k+1} - r_{\hat{x}}^{k+1}) + \widehat{p}_3(s + r_y^{k+1} - r_{\hat{y}}^{k+1}) - q_1(\nabla_y s^k) \\ & - \langle g_1^k, s - s^k \rangle - q_2(\nabla_x f - \nabla_x s^k) - \langle g_2^k, (f - s) - (f - s^k) \rangle + f_k^P(s). \end{aligned}$$

where $f_k^P(s) := \langle s, r_1^{k+1} \rangle + \langle f - s + r_x^{k+1}, r_2^{k+1} \rangle + \langle s + r_y^{k+1}, r_3^{k+1} \rangle + \langle r_z^{k+1}, s - r_z^{k+1} \rangle + \langle r_{\hat{x}}^{k+1}, f - s + r_x^{k+1} - r_{\hat{x}}^{k+1} \rangle + \langle r_{\hat{y}}^{k+1}, s + r_y^{k+1} - r_{\hat{y}}^{k+1} \rangle$. Then at the k th iteration of the PMM algorithm, the actual problem we solve is

$$s^{k+1} = \arg \min_s \{f_k(s)\}.$$

For the proof of the convergence theory, we must first prove the sufficiently decent property of the sequence $\{g(s^k)\}$.

Lemma 1 *Let $\{s^k\}$ be a sequence generated by the PMM algorithm. We have the following descent property*

$$g(s^k) \geq g(s^{k+1}) + \frac{1}{4\tilde{\sigma}_k} \|s^{k+1} - s^k\|^2.$$

Proof Firstly, one can easily prove that the function p_i ($i = 1, 2$ or 3) satisfies

$$|p_i(s_1) - p_i(s_2)| \leq p_i(s_1 - s_2), \quad \forall s_1, s_2 \in \mathbb{R}^{m \times n}. \quad (18)$$

Then, by (18) we have

$$\begin{aligned} f_k(s^k) &= g(s^k) + p_1(s^k - r_z^{k+1}) - p_1(s^k) + p_2(f - s^k + r_x^{k+1} - r_{\hat{x}}^{k+1}) - p_2(f - s^k) \\ &\quad + p_3(s^k + r_y^{k+1} - r_{\hat{y}}^{k+1}) - p_3(s^k) + \frac{1}{2\tilde{\sigma}_k} \|r_z^{k+1}\|^2 + f_k^P(s^k), \\ &\leq g(s^k) + p_1(r_z^{k+1}) + p_2(r_x^{k+1} - r_{\hat{x}}^{k+1}) + p_3(r_y^{k+1} - r_{\hat{y}}^{k+1}) + \frac{1}{2\tilde{\sigma}_k} \|r_z^{k+1}\|^2 \\ &\quad + \text{pert}(r^{k+1}). \end{aligned} \quad (19)$$

In addition, since q_i ($i = 1, 2, 3$) is a convex function and s^{k+1} is a minimizer of the function f_k , we have

$$\begin{aligned} f_k(s^k) &\geq f_k(s^{k+1}) \\ &\geq p_1(s^k - r_z^{k+1}) + \frac{1}{2\tilde{\sigma}_k} \|s^{k+1} - s^k\|^2 - q_1(\nabla_y s^{k+1}) + \\ &\quad p_2(f - s^{k+1} + r_x^{k+1} - r_{\hat{x}}^{k+1}) - q_2(\nabla_x f - \nabla_x s^{k+1}) + p_3(s^{k+1} + r_y^{k+1} - r_{\hat{y}}^{k+1}) \\ &\quad - q_3(h(s^{k+1})), \\ &\geq g(s^{k+1}) - p_1(r_z^{k+1}) - p_2(r_x^{k+1} - r_{\hat{x}}^{k+1}) - p_3(r_y^{k+1} - r_{\hat{y}}^{k+1}) + \frac{1}{2\tilde{\sigma}_k} \|s^{k+1} - s^k\|^2. \end{aligned} \quad (20)$$

The last inequality in (20) is according to (18). In combination of (19) and (20), we obtain

$$\begin{aligned} g(s^k) &\geq g(s^{k+1}) - 2p_1(r_z^{k+1}) - 2p_2(r_x^{k+1} - r_{\hat{x}}^{k+1}) - 2p_3(r_y^{k+1} - r_{\hat{y}}^{k+1}) - \frac{1}{2\tilde{\sigma}_k} \|r_z^{k+1}\|^2 \\ &\quad - \text{pert}(r^{k+1}) + \frac{1}{2\tilde{\sigma}_k} \|s^{k+1} - s^k\|^2. \end{aligned} \quad (21)$$

According to the condition (17), we get the result of this lemma.

In the following, we present the result about the criterion of being a d -stationary point. But before that, we give a definition of a function. For $\tilde{s} \in \mathbb{R}^{m \times n}$, $\tilde{\sigma} > 0$,

$$\begin{aligned} \widehat{f}(s; \tilde{s}, \tilde{\sigma}) := & p_1(s) + p_2(f - s) + p_3(s) - q_1(\nabla_y \tilde{s}) - \langle \nabla_y^* \nabla q_{\alpha, \lambda_1}(\nabla_y \tilde{s}), s - \tilde{s} \rangle - \\ & q_{\alpha, \lambda_2}(\nabla_x(f - \tilde{s})) - \langle \nabla_x^* \nabla q_{\alpha, \lambda_2}(\nabla_x f - \nabla_x \tilde{s}), s - \tilde{s} \rangle \\ & - q_{\alpha, \lambda_3}(h(\tilde{s})) - \langle \nabla q_{\alpha, \lambda_3}(h(\tilde{s})), h(s) - h(\tilde{s}) \rangle + \frac{1}{2\tilde{\sigma}} \|s - \tilde{s}\|^2. \end{aligned}$$

Then in order to prove the result, we need a lemma. Since it is very similar to [8, Lemma 5, Lemma6], we present it without proof.

Lemma 2 *Let $\bar{s} \in \mathbb{R}^{m \times n}$, then \bar{s} is a d -stationary point of (5) if and only if there exist $\tilde{\sigma} \geq 0$ such that \bar{s} is a solution of the following minimization problem*

$$\min_{s \in \mathbb{R}^{m \times n}} \left\{ \widehat{f}(s; \bar{s}, \tilde{\sigma}) \right\}.$$

Now we present the convergence result of the PMM algorithm.

Theorem 2 *Assume that the objective function in (5) is bounded below and $\{\tilde{\sigma}_k\}$ are positive convergent sequences. Then every cluster point of the sequence $\{s^k\}$ generated by the PMM algorithm is a d -stationary point of (5).*

Proof It is known from Lemma 1 that $\{g(s^k)\}$ is a non-increasing sequence. By the assumption that the value of $g(s)$ is bounded below, we obtain that $\{g(s^k)\}$ converges. Meanwhile, $\lim_{k \rightarrow \infty} \|s^{k+1} - s^k\| = 0$. Let $\{s^k\}_{k \in \mathcal{K}}$ be a subsequence of $\{s^k\}$, and $\lim_{k(\in \mathcal{K}) \rightarrow \infty} s^k = s^\infty$. In the following, we prove that s^∞ is a d -stationary point of (5).

Since s^{k+1} is a minimizer of the function f_k , we have

$$\begin{aligned} & \widehat{f}(s; s^k, \tilde{\sigma}_k) + p_1(r_z^{k+1}) + p_2(r_x^{k+1} - r_{\hat{x}}^{k+1}) + p_3(r_y^{k+1} - r_{\hat{y}}^{k+1}) + \frac{1}{2\tilde{\sigma}_k} \|r_z^{k+1}\|^2 \\ & - \langle g_1^k, r_z^{k+1} \rangle + \langle g_2^k, r_x^{k+1} - r_{\hat{x}}^{k+1} \rangle - \langle |\nabla q_3(h(s^k))|, h(r_y^{k+1} - r_{\hat{y}}^{k+1}) \rangle \\ \geq & f_k(s) \geq f_k(s^{k+1}) \\ \geq & \widehat{f}(s^{k+1}; s^k, \tilde{\sigma}_k) - p_1(r_z^{k+1}) - p_2(r_x^{k+1} - r_{\hat{x}}^{k+1}) - p_3(r_y^{k+1} - r_{\hat{y}}^{k+1}) - \frac{1}{2\tilde{\sigma}_k} \|r_z^{k+1}\|^2 \\ & + \langle g_1^k, r_z^{k+1} \rangle - \langle g_2^k, r_x^{k+1} - r_{\hat{x}}^{k+1} \rangle + \langle |\nabla q_3(h(s^k))|, h(r_y^{k+1} - r_{\hat{y}}^{k+1}) \rangle, \forall s \in \mathbb{R}^{m \times n}. \end{aligned}$$

We assume $\lim_{k \rightarrow \infty} \tilde{\sigma}_k = \tilde{\sigma}_\infty$. Note that $\|r^{k+1}\| \rightarrow 0$ due to (17) and h is a continuous function. Then letting $k(\in \mathcal{K}) \rightarrow \infty$, we derive

$$\widehat{f}(s; s^\infty, \tilde{\sigma}_\infty) \geq \widehat{f}(s^\infty; s^\infty, \tilde{\sigma}_\infty), \forall s^\infty \in \mathbb{R}^{m \times n}.$$

Hence, by Lemma 2 we can get the desired result of this theorem.

Finally, we establish the local convergence rate of the sequence $\{s^k\}$ in the following. But before that, we present a lemma.

Lemma 3 In \mathbb{R}^m , define a function $w : \mathbb{R}^m \rightarrow \mathbb{R}$, $w(x_v) := \|x_v\|$, then there is a constant $\kappa \geq 0$ such that

$$\partial w(x_v) \subseteq \partial w(\bar{x}_v) + \kappa \|x_v - \bar{x}_v\| \mathbb{B}_m, \quad \forall x_v \in \mathbb{R}^m. \quad (22)$$

Proof We discuss this problem in three cases:

- (i). If $x_v \neq 0$ and $\bar{x}_v \neq 0$, then $\partial w(x_v) = \left\{ \frac{x_v}{\|x_v\|} \right\}$, $\partial w(\bar{x}_v) = \left\{ \frac{\bar{x}_v}{\|\bar{x}_v\|} \right\}$, we can see that the Lipschitz continuity holds, which implies that the result (22) holds.
- (ii). If $x_v \neq 0$ and $\bar{x}_v = 0$, then $\partial w(x_v) = \left\{ \frac{x_v}{\|x_v\|} \right\}$, $\partial w(\bar{x}_v) = \mathbb{B}_m$, the result (22) obviously holds.
- (iii). If $x_v = 0$ and $\bar{x}_v \neq 0$, then $\partial w(x_v) = \mathbb{B}_m$, $\partial w(\bar{x}_v) = \left\{ \frac{\bar{x}_v}{\|\bar{x}_v\|} \right\}$, therefore (22) holds with $\kappa \geq \frac{1}{\|x_v - \bar{x}_v\|}$.

Theorem 3 Assume that the objective function in (5) is bounded below. Let $\{s^k\}$ be the sequence generated by the PMM algorithm with \mathcal{C}^∞ as the set of all its cluster points. The whole sequence $\{s^k\}$ converges to an element of \mathcal{C}^∞ , if one of the following conditions holds:

- (I) The set \mathcal{C}^∞ contains an isolated element;
- (II) $\{s^k\}$ is a bounded sequence.

Furthermore, based on the condition (II), let $\lim_{k \rightarrow \infty} s^k = s^\infty \in \mathcal{C}^\infty$ and the function g satisfies the KL property at s^∞ with an exponent $\gamma \in [0, 1)$, we have

- (a) The sequence $\{s^k\}$ converges in a finite number of steps, if $\gamma = 0$;
- (b) The sequence $\{s^k\}$ converges R -linearly, i.e., there exist $\mu > 0$ and $\theta \in [0, 1)$ such that $\|s^k - s^\infty\| \leq \mu \theta^k$, if $0 < \gamma \leq \frac{1}{2}$ and k is sufficiently large;
- (c) The sequence $\{s^k\}$ converges R -sublinearly, i.e., there exists $\mu > 0$ such that $\|s^k - s^\infty\| \leq \mu k^{-\frac{1-\gamma}{2\gamma-1}}$, if $\frac{1}{2} < \gamma < 1$ and k is sufficiently large.

Proof Since the objective function in (5) is bounded below, it follows from the proof of Theorem 2 that $\lim_{k \rightarrow \infty} \|s^{k+1} - s^k\| = 0$. Under condition (I), the sequence converges to the isolated element of \mathcal{C}^∞ due to [10, Proposition 8.3.10]. To prove the sequential convergence of $\{s^k\}$ under the condition (II), it suffices to prove the following three properties of $\{s^k\}$ and then apply the convergence results in [2, Theorem 2.9] to the function g :

- (i) The sequence $\{g(s^k)\}$ is descent, i.e., $g(s^{k+1}) \geq g(s^k) + \frac{c}{2} \|s^{k+1} - s^k\|^2$, $\forall k \geq 1$, where $c > 0$ is a constant;
- (ii) There exists a subsequence $\{s^k\}_{k \in \mathcal{K}}$ of $\{s^k\}$ such that $\lim_{k(\in \mathcal{K}) \rightarrow \infty} s^k = s^\infty$

and $\lim_{k(\in \mathcal{K}) \rightarrow \infty} g(s^k) = g(s^\infty)$;

- (iii) There exist a constant $K > 0$ and $\varepsilon^{k+1} \in \partial g(s^{k+1})$ such that $\|\varepsilon^{k+1}\| \leq K \|s^{k+1} - s^k\|$, for k sufficiently large.

Obviously, the first two properties have been proven. Now we focus on the proof of the third property. Let

$$\bar{\varepsilon}^{k+1} := g_1^k - g_1^{k+1} - g_2^k + g_2^{k+1} - \frac{1}{\bar{\sigma}_k} (s^{k+1} - s^k - r_z^{k+1}) - r_1^{k+1} - r_z^{k+1}.$$

Then $\bar{\varepsilon}^{k+1} \in \partial g_k(s^{k+1})$, where

$$g_k(s) = p_1(s - r_z^{k+1}) + p_2(f - s + r_x^{k+1} - r_{\hat{x}}^{k+1}) + p_3(s + r_y^{k+1} - r_{\hat{y}}^{k+1}) \\ - q_{\alpha, \lambda_1}(\nabla_y s) - q_{\alpha, \lambda_2}(\nabla_x f - \nabla_x s) - q_{\alpha, \lambda_3}(h(s + r_y^{k+1} - r_{\hat{y}}^{k+1})).$$

According to the special structure of the function h , we may consider every element h_i separately. Since the functions ∂p_1 and ∂p_2 are piecewise polyhedral, $\|r_z^{k+1}\|$ and $\|r_x^{k+1} - r_{\hat{x}}^{k+1}\|$ are sufficiently small for all k sufficiently large, we can deduce from [15] that ∂p_1 and ∂p_2 are locally upper Lipschitz continuous. Hence, it is known from Lemma 3 and [16, Theorem 23.8] that there exist $\kappa_1, \kappa_2, \kappa_3 \geq 0$, such that

$$\begin{aligned} \bar{\varepsilon}^{k+1} &\in \partial p_1(s^{k+1} - r_z^{k+1}) + \partial p_2(f - s^{k+1} + r_x^{k+1} - r_{\hat{x}}^{k+1}) + \\ &\quad \partial p_3(s^{k+1} + r_y^{k+1} - r_{\hat{y}}^{k+1}) - \partial q_{\alpha, \lambda_3}(h(s^{k+1} + r_y^{k+1} - r_{\hat{y}}^{k+1})) - g_1^{k+1} + g_2^{k+1} \\ &\subset \partial p_1(s^{k+1}) + \kappa_1 \|r_z^{k+1}\| \mathbb{B}_{m \times n} + \partial p_2(f - s^{k+1}) + \kappa_2 \|r_x^{k+1} - r_{\hat{x}}^{k+1}\| \mathbb{B}_{m \times n} \\ &\quad + \partial p_3(s^{k+1}) - \partial q_{\alpha, \lambda_3}(h(s^{k+1})) + \kappa_3 \|r_y^{k+1} - r_{\hat{y}}^{k+1}\| \mathbb{B}_{m \times n} - g_1^{k+1} + g_2^{k+1} \\ &= \partial p_1(s^{k+1}) + \partial p_2(f - s^{k+1}) + \partial p_3(s^{k+1}) - \partial q_{\alpha, \lambda_3}(h(s^{k+1})) + (\kappa_1 \|r_z^{k+1}\| \\ &\quad + \kappa_2 \|r_x^{k+1} - r_{\hat{x}}^{k+1}\| + \kappa_3 \|r_y^{k+1} - r_{\hat{y}}^{k+1}\|) \mathbb{B}_{m \times n} - g_1^{k+1} + g_2^{k+1}. \end{aligned}$$

Hence, we can find $d\bar{\varepsilon}^{k+1} \in \mathbb{R}^{m \times n}$ with $\|d\bar{\varepsilon}^{k+1}\| \leq \kappa_1 \|r_z^{k+1}\| + \kappa_2 \|r_x^{k+1} - r_{\hat{x}}^{k+1}\| + \kappa_3 \|r_y^{k+1} - r_{\hat{y}}^{k+1}\|$, such that $\varepsilon^{k+1} := \bar{\varepsilon}^{k+1} + d\bar{\varepsilon}^{k+1} \in \partial g(s^{k+1})$. From (17), we know that there exists a constant $\kappa_4 > 0$, such that $\|d\bar{\varepsilon}^{k+1}\| \leq \kappa_4 \|s^{k+1} - s^k\|$. In combination of (17) and the Lipschitz continuity of $\nabla_y^* \nabla q_{\alpha, \lambda_1}$ and $\nabla_x^* \nabla q_{\alpha, \lambda_2}$, we can find some $\kappa_5 > 0$, such that $\|\bar{\varepsilon}^{k+1}\| \leq \kappa_5 \|s^{k+1} - s^k\|$. Therefore, we can get the result of (iii). Finally, since we have proved the properties (i)-(iii), the results for the convergence rate can be established similar to [1, Theorem 2] or [3, Proposition 4].

5 Numerical Experiments

In this section, we implement some numerical experiments to demonstrate the efficiency of our algorithm. All the experiments are conducted on a Desktop with Intel(R) Core(TM) i5-8250U, CPU@1.60GHz of 8G memory running 64 bit Windows operation system. All the codes are written in MATLAB (R2018a) with some subroutines written in C.

In order to give an overall evaluation, we select the full-reference evaluation indices: the peak signal-to-noise ratio (PSNR) and the structural similarity (SSIM) [20], which are defined as follows.

Definition 2 (Peak Signal-to-noise Ratio (PSNR)) Given a clean image u and a degraded image v of $m \times n$, the PSNR is defined as

$$\text{PSNR} := 10 \log_{10} \left(\frac{u_{\max}^2}{\text{MSE}} \right),$$

where MSE denotes the mean square error and is defined as

$$\text{MSE} := \frac{1}{mn} \sum_{i=1}^m \sum_{j=1}^n (u_{ij} - v_{ij})^2.$$

Definition 3 (Structural Similarity (SSIM) [20]) The mean values of the images u and v are denoted as

$$\mu_u = \frac{1}{mn} \sum_{i=1}^m \sum_{j=1}^n u_{ij}$$

and

$$\mu_v = \frac{1}{mn} \sum_{i=1}^m \sum_{j=1}^n v_{ij},$$

respectively. The standard deviations are denoted as

$$\sigma_u = \left(\frac{1}{mn-1} \sum_{i=1}^m \sum_{j=1}^n (u_{ij} - \mu_u)^2 \right)^{\frac{1}{2}}$$

and

$$\sigma_v = \left(\frac{1}{mn-1} \sum_{i=1}^m \sum_{j=1}^n (v_{ij} - \mu_v)^2 \right)^{\frac{1}{2}},$$

respectively. The covariance of the images u and v is denoted as

$$\sigma_{uv} = \frac{1}{mn-1} \sum_{i=1}^m \sum_{j=1}^n (u_{ij} - \mu_u)(v_{ij} - \mu_v).$$

And the factors of the luminance, contrast, and structure of the images u and v are defined as

$$l(u, v) := \frac{2\mu_u\mu_v + c_1}{\mu_u^2 + \mu_v^2 + c_1}, \quad c(u, v) := \frac{2\sigma_u\sigma_v + c_2}{\sigma_u^2 + \sigma_v^2 + c_2}, \quad s(u, v) := \frac{\sigma_{uv} + c_3}{\sigma_u\sigma_v + c_3},$$

where $c_1 = (k_1 L_u)^2$, $c_2 = (k_2 L_u)^2$, $c_3 = c_2/2$ are three constants. $k_1 = 0.01$ and $k_2 = 0.03$ are the common default values. Then we can define

$$\text{SSIM} := [l(u, v)]^\alpha [c(u, v)]^\beta [s(u, v)]^\gamma.$$

In order to simplify the expression, we set $\alpha, \beta, \gamma = 1$ in this paper, then we have

$$\text{SSIM} = \frac{(2\mu_u\mu_v + c_1)(2\sigma_{uv} + c_2)}{(\mu_u^2 + \mu_v^2 + c_1)(\sigma_u^2 + \sigma_v^2 + c_2)}.$$

For the nonconvex model, the iteration process of the outer problem is terminated if

$$\max\{R_p^k, R_d^k\} < \text{To1} = 2 \times 10^{-4}$$

is satisfied, where

$$R_p^k = \frac{\|f - s^k - u^k\| + \|s^k - v^k\|}{1 + \|f\|},$$

$$R_d^k = \frac{\| -x^k - \hat{x}^k \| + \| -x^k + y^k - z^k \| + \| -y^k - \hat{y}^k \|}{1 + \|f\|},$$

or the iteration number reaches 5. The iteration process of the subproblem is terminated if

$$2p_1(r_z^{k+1}) + 2p_2(r_x^{k+1} - r_{\hat{x}}^{k+1}) + 2p_3(r_y^{k+1} - r_{\hat{y}}^{k+1}) + \frac{1}{2\tilde{\sigma}_k} \|r_z^{k+1}\|^2 + \text{pert}(r^{k+1}) \leq \frac{1}{4\tilde{\sigma}_k} \|s^{k+1} - s^k\|^2,$$

or the iteration number reaches 100.

For the convex model, the iteration process is terminated if

$$\max\{R_p^k, R_d^k, R_c^k\} < \text{To1} = 2 \times 10^{-4}$$

is satisfied, where

$$R_p^k = \frac{\|f - s^k - u^k\| + \|s^k - v^k\|}{1 + \|f\|},$$

$$R_d^k = \frac{\| -x^k - \hat{x}^k \| + \| -x^k + y^k - z^k \| + \| -y^k - \hat{y}^k \|}{1 + \|f\|},$$

$$R_c^k = \frac{\|s^k - \text{Prox}_{\hat{p}_1}(s^k + z^k)\| + \|u^k - \text{Prox}_{p_2}(u^k + \hat{x}^k)\| + \|v - \text{Prox}_{\hat{p}_3}(v^k + \hat{y}^k)\|}{1 + \|f\|},$$

or the iteration number reaches 500.

Three real remote sensing stripe images with different stripe noise distributions are downloaded from the website <https://ladsweb.nascom.nasa.gov/>. Although there are three parameters in the model (3) and (4), we only need to do the cross validation for two parameters by dividing one parameter.

In Table 1, we present the experimental results of different algorithms on the convex model and the nonconvex model, respectively. The image is degraded by nonperiodical and periodical stripes, respectively. From the table, we can see that the nonconvex model performs better than the convex counterpart, especially for the PSNR. In addition, for the convex model, the dADMM performs better than the pADMM. This also demonstrates that we adopt the dADMM to solve the subproblems of the PMM is reasonable.

Furthermore, we also present the stripe and destripe images in Figures 1-3 to illustrate the effectiveness of the model. We can see that the proposed model can remove the stripes, and preserve the stripe-free information and the image details very well.

Table 1 Experimental results

Stripe noise	Case	Index	Degraded	Convex model		Nonconvex model
				pADMM	dADMM	
Nonperiodical	Case 1	KKT		1.99e-4	1.99e-4	1.99e-4
		PSNR	23.05	55.47	59.13	63.36
		SSIM	0.6486	0.9995	0.9998	0.9999
		time iter		26.89 478	21.48 233	39.24 434
	Case 2	KKT		1.99e-4	1.98e-4	1.99e-4
		PSNR	18.27	53.92	58.78	62.43
		SSIM	0.2753	0.9995	0.9997	0.9998
		time iter		24.38 401	17.56 218	33.21 382
	Case 3	KKT		1.99e-4	1.99e-4	2.00e-4
PSNR		24.33	43.67	48.82	55.38	
SSIM		0.3626	0.9943	0.9962	0.9976	
time iter			18.46 378	13.39 179	30.25 352	
Periodical	Case 1	KKT		1.99e-4	2.00e-4	2.00e-4
		PSNR	20.68	52.00	57.13	62.00
		SSIM	0.5868	0.9987	0.9995	0.9999
		time iter		37.64 492	29.12 281	55.83 500
	Case 2	KKT		1.99e-4	1.99e-4	1.79e-4
		PSNR	17.67	40.75	46.69	54.42
		SSIM	0.4577	0.9946	0.9960	0.9992
		time iter		16.57 455	11.28 180	28.26 440
	Case 3	KKT		1.98e-4	1.99e-4	1.96e-4
PSNR		18.32	41.05	48.36	55.98	
SSIM		0.3283	0.9949	0.9970	0.9995	
time iter			14.25 423	9.98 167	25.76 409	

6 Conclusion

In this paper, we have developed a nonconvex model for remote sensing stripe images. For the computational issues, we have applied the inexact PMM algorithm to solve the model with the inner subproblem solved by the dADMM. Meanwhile, we have analyzed the convergence of the algorithm based on the KL property. Finally, numerical experiments demonstrate the superiority of the proposed model and algorithm.

References

1. Attouch, H., Bolte, J.: On the convergence of the proximal algorithm for nonsmooth functions involving analytic features. *Mathematical Programming* **116**, 5–16 (2009)
2. Attouch, H., Bolte, J., Svaiter, B.: Convergence of descent methods for semi-algebraic and tame problems: proximal algorithms, forward-backward splitting, and regularized gauss-seidel methods. *Mathematical Programming* **137**, 91–129 (2013)
3. Bolte, J., Pauwels, E.: Majorization-minimization procedures and convergence of sqp methods for semi-algebraic and tame programs. *Mathematics of Operations Research* **41**(2), 442–465 (2016)

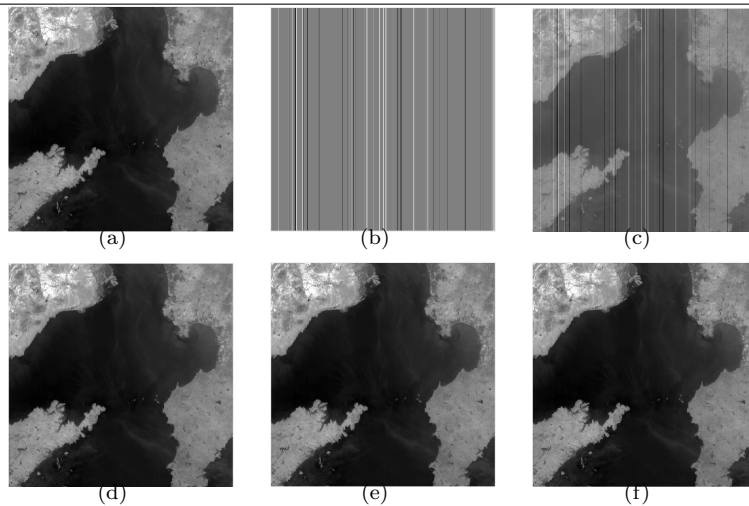


Fig. 1 The destriping results. (a) Original image; (b) stripe component; (c) degraded image; (d) estimated image by the convex model (pADMM); (e) estimated image by the convex model (dADMM); (f) estimated image by the nonconvex model

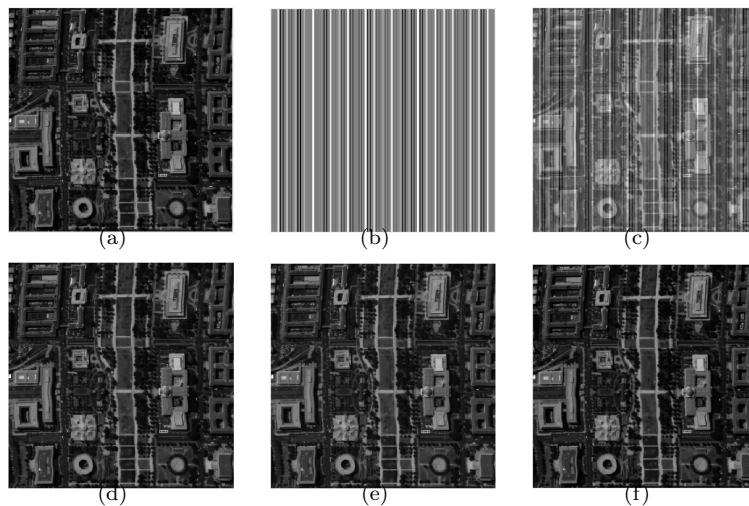


Fig. 2 The destriping results. (a) Original image; (b) stripe component; (c) degraded image; (d) estimated image by the convex model (pADMM); (e) estimated image by the convex model (dADMM); (f) estimated image by the nonconvex model

4. Bouali, M., Ladjal, S.: Toward optimal destriping of MODIS data using a unidirectional variational model. *IEEE Transactions on Geoscience and Remote Sensing* **49**(8), 2924–2935 (2011)
5. Chen, L., Sun, D.F., Toh, K.C.: An efficient inexact symmetric gauss-seidel based majorized admm for high-dimensional convex composite conic programming. *Mathematical Programming* **161**, 237–270 (2017)
6. Chen, Y., Huang, T.Z., Deng, L.J., Zhao, X.L., Wang, M.: Group sparsity based regularization model for remote sensing image stripe noise removal. *Neurocomputing* **267**, 95–106 (2017)

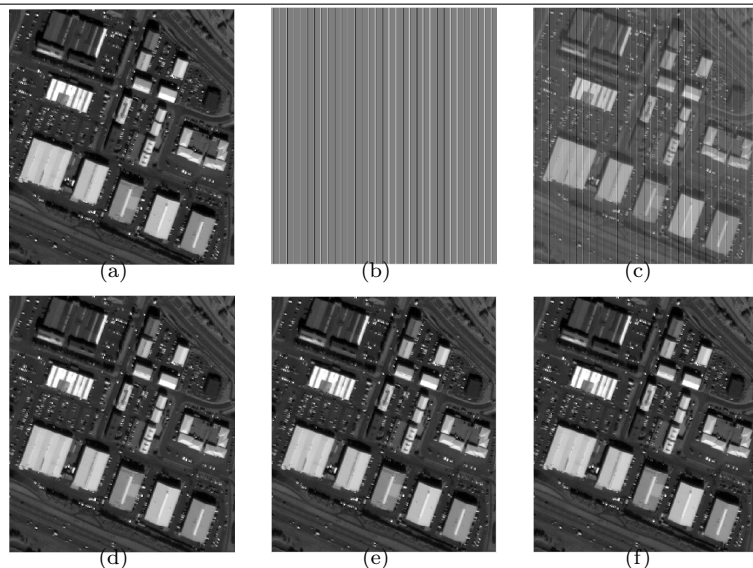


Fig. 3 The destriping results. (a) Original image; (b) stripe component; (c) degraded image; (d) estimated image by the convex model (pADMM); (e) estimated image by the convex model (dADMM); (f) estimated image by the nonconvex model

7. Condat, L.: A direct algorithm for 1d total variation denoising. *IEEE Signal Processing Letters* **20**(11), 1054–1057 (2013)
8. Cui, Y., Pang, J., Sen, B.: Composite difference-max programs for modern statistical estimation problems. *SIAM Journal on Optimization* **28**(4), 3344–3374 (2018)
9. Du, B., Zhang, L., Tao, D., Zhang, D.: Unsupervised transfer learning for target detection from hyperspectral images. *Neurocomputing* **120**, 72–82 (2013)
10. Facchinei, F., Pang, J.S.: *Finite-Dimensional Variational Inequalities and Complementarity Problems*. Springer New York (2003)
11. Fan, J., Li, R.: Variable selection via nonconcave penalized likelihood and its oracle properties. *Journal of the American Statistical Association* **96**(456), 1348–1360 (2017)
12. Huang, H., Huang, Y.: Improved discriminant sparsity neighborhood preserving embedding for hyperspectral image classification. *Neurocomputing* **136**, 224–234 (2014)
13. Huang, H., Tang, Y., Tan, Z., Zhuang, J., Hou, C., Chen, W., Ren, J.: Object-based attention mechanism for color calibration of UAV remote sensing images in precision agriculture. *IEEE Transactions on Geoscience and Remote Sensing* **60**, 1–13 (2022)
14. Richards, J.A.: *Remote Sensing Digital Image Analysis*, 6th edn. Springer (2022)
15. Robinson, S.: Some continuity properties of polyhedral multifunctions. *Mathematical Programming Study* **14**, 206–214 (1981)
16. Rockafellar, R.: *Convex Analysis*. Princeton University Press (1970)
17. Shen, H., Zhang, L.: A map-based algorithm for destriping and inpainting of remotely sensed images. *IEEE Transactions on Geoscience and Remote Sensing* **47**(5), 1492–1502 (2009)
18. Tang, P., Wang, C., Jiang, B.: A proximal-proximal majorization-minimization algorithm for nonconvex rank regression problems. to appear in *Journal of Scientific Computing* (2021)
19. Tang, P., Wang, C., Sun, D., Toh, K.C.: A sparse semismooth newton based proximal majorization-minimization algorithm for nonconvex square-root-loss regression problems. *Journal of Machine Learning Research* **21**, 1–38 (2020)
20. Wang, Z., Bovik, A.C., Sheikh, H.R., Simoncelli, E.P.: Image quality assessment: From error visibility to structural similarity. *IEEE Transactions on Image Processing* **13**(4), 600–612 (2004)

-
21. Zhou, G., Chen, W., Gui, Q., Li, X., Wang, L.: Split depth-wise separable graph-convolution network for road extraction in complex environments from high-resolution remote-sensing images. *IEEE Transactions on Geoscience and Remote Sensing* **60**, 1–15 (2022)